論文の内容の要旨

論文題目　Study on External-Field-Induced Novel Fabrication Processes of Organic Field-Effect Transistors
（外場印加による有機トランジスタ作製の新規プロセスに関する研究）

氏名　小槻 賢志

Introduction

Organic field effect transistors (OFETs) have attracted much attention for next generation devices. Based on recent developments of fabrication techniques, OFETs with high mobility over 10 cm^2/Vs have been reported. To obtain a semiconductor film with high crystallinity and intentional orientation, pre-patterned templates have been widely used for vapor and solution growth. Application of external field, on the other hand, also has possibility for controlling crystal growth. So far, applications of light, electric field, magnetic field and mechanical vibration have been performed during an OFET fabrication process. If such an external field can be combined with conventional fabrication techniques, it will be another potential way for OFET fabrications. I fabricated OFETs with external fields in three schemes as follows.

Scheme 1. Electric-Field-Assisted Fabrication of Pentacene Single Crystal FETs during Drop-Casting

Application of electric field during organic crystal's growth has been mainly performed for vapor growth. In vapor growth, electric field interacts with molecular dipole moment and affects the molecular orientation. However, the interaction between molecules and substrates is often larger than that of molecules and electric field, which limited the effects of electric field within small crystallites. To control crystal growth in a macroscopic scale, application of electric field during solution process is desirable. In this scheme, I applied electric field during a drop-casting process to obtain pentacene single-crystal (SC) OFETs.

The process was schematically illustrated in Figure 1a,b. In this scheme, reduced graphene oxide (RGO) electrodes were fabricated on an SiO_2/Si substrate by spin-coating GO solution and subsequent annealing at 500 °C. Then 0.025 wt.% solution of pentacene in 1,2,4-trichlorobenzene at 200 °C was drop-cast on the substrate kept at 130 °C under a N_2 atmosphere in a glovebox. Immediately after the drop-cast, pentacene microcrystals appeared in the liquid by rapid cooling and their size continued to increase approximately for 20 s (Figure1b). Then the electric field was applied. Solvent evaporated gradually and finally disappeared after 300 s.

At first, direct current (DC) electric field was applied between two electrodes. When electric field of larger than 1.0×10^5 V/m was applied, pentacene microcrystals flowing in liquid immediately captured to the cathode. Increasing the electric field up to 1.4×10^6 V/m, quantity of captured SCs were increased further. In the case of DC field, however, most of SCs were captured only at cathode. Next, to place pentacene SCs between two electrodes and form an OFET configuration, alternating current (AC) electric field was applied. Under AC electric field, SCs swung over channel according to the applied strength and frequency. The real-time observation reveals the vibration amplitude was dependent on electric field's strength, and swinging frequency was also dependent on applying frequency. By optimizing strength and frequency as 1.5×10^5 V/m and 100 Hz, pentacene SCs were successfully placed automatically between electrodes as Figure 2d.

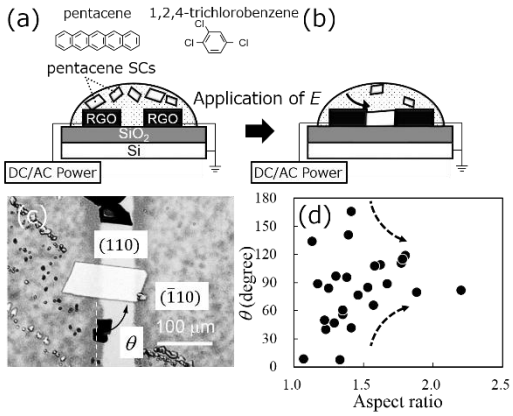

Figure 1. (a,b) Schematic illustration of the process. (c) Optical image of a pentacene single crystal automatically placed between electrodes. (d) Crystallographic orientation of pentacene crystals as a function of aspect ratio.

These results indicates pentacene SCs experienced positive electrification and electrophoresis in solution. As a pentacene SC itself is intrinsically neutral, this positive charge is caused by the contact with surrounding solvent according to Coehn's rule. Besides, crystallographic orientation of obtained SCs shows dependence on their aspect ratio (length ratio of long axis to short one). That is, SCs with aspect ratio larger than 1.5 tended to align perpendicular to the channel (Figure 2e). As the rotation is known to be caused by the interaction between electric field and induced dipole moment in a crystal, the present result suggested that a large aspect ratio induces a large dipole moment. Finally, FET characterization of obtained SCs was performed. Field-effect mobility of most SC-FETs was larger than 0.2 cm^2/Vs, and maximum mobility of 0.49 cm^2/Vs was obtained. In addition, SCs with more perpendicular to the channel tended to show higher mobility, which implied the alignment control by electric field was also important for resulting device performance. Thus, external electric field was revealed to be efficient for facile top-down fabrication of SC-OFETs.

Scheme 2. Electric-Field-Assisted Fabrication of C8-BTBT Single Crystal FETs during Solvent Vapor Annealing

As mentioned in section 1, pentacene SCs can be aligned toward the direction of applied electric field. Although it is a simple fabrication process, pentacene had crystallized before applying electric field, which caused wide distribution of crystal shapes or crystal sizes. To solve these problems, crystallization of organic semiconductor and application of electric field were simultaneously performed during a solvent vapor annealing (SVA) process.

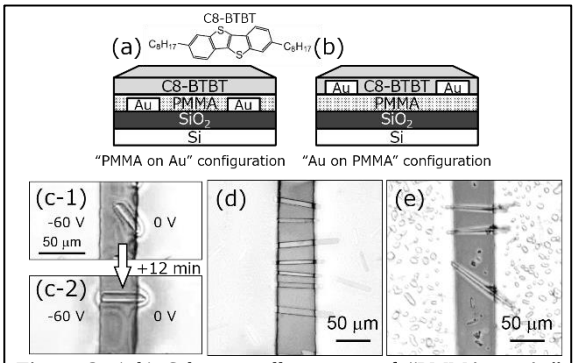

Figure 2. (a,b) Schematic illustrations of "PMMA on Au" configuration (a) and "Au on PMMA" configuration (b). (c) Optical images of "PMMA on Au" configuration under DC electric field during SVA. (d,e) Optical images of "PMMA on Au" (d) and "Au on PMMA" configurations (e) after SVA.

Two kinds of specimens were prepared for the SVA process: a "PMMA on Au" configuration and an "Au on PMMA" configuration as illustrated in Figure 2a,b. In the former configuration, the double layer of dioctyl-benzothienobenzothiophene (C8-BTBT) and poly-methyl methacrylate (PMMA) was formed on an SiO_2/Si substrate with Au electrodes of 35 nm thickness and 50 μm channel length. Mixed solution of C8-BTBT (0.5 wt.%) and PMMA (0.5 wt.%) in chlorobenzene was spin-coated on the substrate. In the latter "Au on PMMA" configuration, on the other hand, 1 wt.% solution of PMMA in chlorobenzene was firstly spin-coated on an SiO_2/Si substrate. Subsequently, Au electrodes (35 nm) were formed in vacuum, and a C8-BTBT layer was formed by spin-coating 1 wt.% solution in toluene. Then, these two kinds of substrates were exposed to chloroform vapor in a Petri dish at room temperature for 40 min. During this SVA process, electric field was applied and crystallization of C8-BTBT SCs was observed by optical microscopy.

In the SVA process, C8-BTBT nucleates in one to two minutes and growing further with a rod-like SC form which is parallel to [100] direction. Figure 2c shows optical images during the SVA process on the "PMMA on Au" configuration. When a DC electric field (1.2×10^6 V/m) was applied to both electrodes, SCs once moved from the cathode to the anode as if they were negatively charged (2c-1). Then, growing SCs rotated toward the direction of the electric field (2c-2). In this way, SCs' displacement and rotation were occurred by electric field, which is similar to Scheme 1. However, unlike the case of positive electrification of pentacene SCs, C8-BTBT SCs were negatively charged. Based on Coehn's rule, this difference might be caused by the large difference of dielectric constant of surrounding solvent. With respect to the crystal rotation, C8-BTBT SCs gradually rotated toward the electric field. As this alignment was caused by the interaction between electric field and induced dipole moment as mentioned in Scheme 1, the dipole moment was gradually strengthened according to the increase of aspect ratio up to 10. In this way, C8-BTBT SCs were successfully placed automatically between two electrodes.

In this "PMMA on Au" configuration, FET performance of obtained devices was very poor (about 0.01 cm^2/Vs) caused by a remaining PMMA layer between SCs and electrodes. To achieve an electrically good contact, the "Au on PMMA" configuration was investigated. In this configuration, unfortunately, SCs were more likely to align perpendicular to the electric field than the former configuration, which was due to the difference of surface wettability and the topographical steps at the channel/electrodes interface. However, a DC electric field (1.2×10^6 V/m) successfully made them parallel to the electric field and contacting both electrodes directly (Figure 2e). The maximum mobility of obtained SC-FETs on this configuration was as high as 1.9 cm^2/Vs. In this way, I successfully fabricated high-performance SC-FETs through a facile but efficient method with electric field.

Scheme 3. Light-Irradiation-Induced Mobility Enhancement of C8-BTBT FETs

In Schemes 1 and 2, electric field was utilized for the SCs' placement. Application of external field as a post-process, on the other hand, has a more fascinating possibility for OFET fabrication, because it can be more easily combined with conventional fabrication techniques. In Scheme 3, a light irradiation as a post-external field was performed on pre-formed C8-BTBT FETs to enhance their performances.

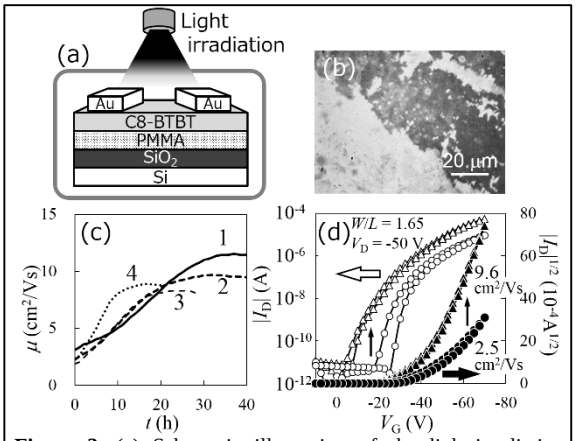

Figure 3. (a) Schematic illustration of the light-irradiating process. (b) Polarized optical image of film before light irradiation. (c) Time dependence of mobility of four samples during light irradiation in the ambient atmosphere. (d) Typical transfer characteristics before (circles) and after (triangles) light irradiation measured in the dark and in a vacuum.

In this scheme, a double layer of C8-BTBT and PMMA was firstly fabricated on an SiO_2/Si substrate by spin-coating a mixed solution of C8-BTBT (0.5 wt.%) and PMMA (1 wt.%) in chlorobenzene. This substrate was put on a hot plate heated at 130 °C beforehand, and then the hot plate was cooled down to room temperature at a cooling rate of about -2 °C/min. Subsequently Au electrodes (20 nm) were deposited on the double layer. Finally, light was irradiated from a metal-halide lamp (1,700 lx) under various atmospheres (air/vacuum/N_2/O_2). During this irradiation, evolution of the FET performance was measured.

In the pre-annealing process, the C8-BTBT film once melted and then recrystallized into the crystalline domains with width of 100 μm as shown in a polarized image (Figure 3b). Throughout this recrystallization, the field-effect mobility increased from 0.2~0.8 cm^2/Vs to 1~3 cm^2/Vs. Subsequent light irradiation improved highly the mobility, the changes of which were summarized in Figure 3c. For all four samples, the mobility was enhanced by light irradiation up to as high as 8~12 cm^2/Vs. To exclude the influence of light on the FET performance, the transfer characteristics before/after the irradiation were measured in the dark and in a vacuum (Figure 3d). As a result, the mobility was found to be intrinsically increased (2.5/9.6 cm^2/Vs), while the threshold voltage (V_T) was almost unchanged (-46/-41 V). Similar mobility enhancement was also observed under the O_2 atmosphere, though it was not observed in a vacuum or under the N_2 atmosphere. In addition, the mobility was not enhanced without light irradiation under any atmospheres.

So far, the effects of light irradiation were mainly focused on the V_T shift, which would sometimes yield an apparent increase of mobility. In the present study, however, the effective enhancement of mobility was also observed in addition to the V_T shift. The FET characteristics measured before/after the irradiation (Figure 3d) revealed that these mobility enhancement and the V_T shift were independent phenomena. Although the V_T shift was known to come from the "temporary" charge traps induced at a semiconductor/insulator interface, the mobility enhancement was supposed to originate from the change which occurred "intrinsically" in the film. This assumption was supported by an X-ray diffraction (XRD) measurement, where a (001) interlayer distance changed from 2.93 nm to 2.90 nm before/after the irradiation. Such compression of the crystal lattice means the π-π interactions between molecules. As the mobility enhancement was observed only under the ambient or O_2 atmosphere, the light-induced interaction with molecules and O_2 will cause the lattice compression. In this way, I successfully achieved the mobility enhancement by post-processing light irradiation.

Conclusion

In this work, external fields were applied for the fabrication of OFETs in three schemes. In Schemes 1 and 2, external electric field was found to induce displacement and rotation of SCs, which were caused by the static electrophoresis and electric-field-induced dipole moment. Based on these effects, pentacene or C8-BTBT SCs were successfully placed automatically between the pre-patterned electrodes, forming a single-crystal OFET structure. In Scheme 3, post-processing light irradiation achieved the enhancement of C8-BTBT FET's mobility up to higher than 10 cm^2/Vs. XRD measurement revealed a compression of the crystal lattice during the irradiation, which induced a closed molecular packing. Application of external field thus proved a promising way for the facile fabrication of high-performance OFETs.